frontiers in Earth Science

ORIGINAL RESEARCH
published: 06 May 2016
doi: 10.3389/feart.2016.00054

Sensitivity of Sediment Magnetic Records to Climate Change during Holocene for the Northern South China Sea

Tingping Ouyang[1, 2], Mingkun Li[1, 3], Xiang Zhao[2], Zhaoyu Zhu[1], Chengjing Tian[1, 4], Yan Qiu[4], Xuechao Peng[4] and Qiao Hu[1]*

[1] Key Laboratory of Marginal Sea Geology, Guangzhou Institute of Geochemistry, Chinese Academy of Sciences, Guangzhou, China, [2] Research School of Earth Sciences, Australian National University, Canberra, ACT, Australia, [3] University of Chinese Academy of Sciences, Beijing, China, [4] Guangzhou Marine Geological Survey, Guangzhou, China

Magnetic property has been proved to be a sensitive proxy to climate change for both terrestrial and marine sediments. Based on the schedule frame established by AMS ^{14}C dating of foraminifera, detail magnetic analyses were performed for core PC24 sediments at sampling intervals of 2 cm to discuss magnetic sensitivity of marine sediment to climate during Holocene for the northern South China Sea. The results indicated that: (1) Concentration dependent magnetic parameters are positive corresponding to variation of temperature. The frequency dependent susceptibility coefficient basically reflected the variation in humidity; (2) χ_{ARM}/SIRM was more sensitive to detrital magnetite particles and SIRM/χ was more effective to bioge χ_{ARM}/SIRM and SIRM/χ are corresponding to precipitation and temperature, respectively; (3) the Holocene Megathermal in the study area was identified as 7.5–3.4 cal. ka BP. The warmest stage of Holocene for the study area should be during 6.1–3.9 cal. ka BP; (4) The 8 ka cold event was characterized as cold and dry during 8.55–8.25 cal. ka BP; (5) During early and middle Holocene, the climate combinations were warm dry and cold wet. It turned to warm and wet after 2.7 cal. ka BP.

Keywords: magnetic properties, sensitivity, climate change, Holocene, the northern South China Sea

OPEN ACCESS

Edited by:
Qingsong Liu,
Chinese Academy of Sciences, China

Reviewed by:
Chuang Xuan,
University of Southampton, UK
Xiaoqiang Yang,
Sun Yat-Sen University, China
Weiguo Zhang,
East China Normal University, China

****Correspondence:***
Tingping Ouyang
oyangtp@gig.ac.cn

Specialty section:
This article was submitted to Geomagnetism and Paleomagnetism, a section of the journal Frontiers in Earth Science

Received: *18 December 2015*
Accepted: *18 April 2016*
Published: *06 May 2016*

Citation:
Ouyang T, Li M, Zhao X, Zhu Z, Tian C, Qiu Y, Peng X and Hu Q (2016) Sensitivity of Sediment Magnetic Records to Climate Change during Holocene for the Northern South China Sea. Front. Earth Sci. 4:54. doi: 10.3389/feart.2016.00054

INTRODUCTION

The South China Sea (SCS), one of the largest margin seas in the world, is located between the Pacific Ocean and the Asian continent. The SCS can be subdivided into northwestern, southwestern, and eastern sub-basins (He and Chen, 1987; Liu, 1992). As the most frequent activity area of East Asian monsoon, it has become a hot area of climate research (Chen et al., 2003; Wei et al., 2006; Wan et al., 2007; Hu et al., 2012). As suggested by Han and Fyfe (1995) and Wang (2009), it is an important place for paleoenvironment and paleoclimate research and can be considered as another natural laboratory besides the Chinese Loess Plateau for the study of regional response to global climate change and its driving forces.

During the last decades, magnetic properties has been proven to be sensitive proxies to climate change and has been widely applied in climatic and environmental evolution research using loess-paleosol sequences, ice cores as well as marine sediments (Moreno et al., 2002; Maher, 2007; Heslop and Roberts, 2013; Zan et al., 2015). Previous studies suggested that marine sediment was one of

the most important signal carriers of climate change. Therefore, marine sediment magnetic records have been becoming another focus of paleaoclimate research (Arai et al., 1997; Kissel et al., 1999; Oldfield et al., 2003; Tang et al., 2003; Kumar et al., 2005; Sangode et al., 2007; Xu et al., 2011; Larrasoaña et al., 2015). Many magnetic results of the SCS sediments were reported since the past decade. However, previous research indicated that sediment magnetic response to climate change varied much among different regions within the South China Sea (SCS) (Wang et al., 1993; Hou et al., 1996; Kissel et al., 2003; Yim et al., 2004; Yang et al., 2007; Ouyang et al., 2014a). Zhang et al. (2010) compared many cores within the SCS and pointed out that the SCS could be divided into at least two regions according to variation characteristics of magnetic susceptibility. Magnetic susceptibility (MS) varied parallel with the calcium carbonate percent content and foraminifera $\delta^{18}O$ curves during late Quaternary at the region close to Dongsha Islands. However, a mirror image relationship was appeared between variation of magnetic susceptibility and calcium carbonate percent content during late Quaternary at western and southern SCS. Many factors such as water depth and early diagenesis can affect the MS variation characteristics. In addition, different climate change response might play more important role on sediments magnetic properties. For example, previous comparison between DP1144 and ODP1143 indicated that different climate change response was appeared between the northern and southern SCS (Jin and Jian, 2008).

In the present study, a detailed environmental magnetic analysis was performed for a sediment core PC24 collected from the northern SCS. Our main aim is to identify the dynamic of sediment magnetic variation and it sensitivity and magnetic response to climate change during Holocene for the northern SCS.

MATERIALS AND METHODS

Sampling and Geological Background

The 7.6-m-long piston core (PC24) studied here was recovered by the Guangzhou Marine Geological Survey in June, 2008, from the northwestern sub-basin (latitude/longitude: 17.4°N, 113.7°E) at a water depth of 3433 m (**Figure 1**). The recovered sediments consist of clayey silts that are yellow-gray and gray in the upper 1.01 m and gray from 1.01 to 7.6 m. Occasional fine yellow sand layers are preserved throughout the core. The studied core was split and one half was continuously sampled by inserting plastic cubes ($2 \times 2 \times 2$ cm^3) into the split face of core sections. Sediment at the base of each cube was then cut away with a non-magnetic knife, and the cubes were sealed with plastic end-pieces and clear polyethylene tape. In total, 380 magnetic samples were taken, along with bulk sediment samples at the same depths.

We attempted to extract foraminifera from the sediment to obtain a $\delta^{18}O$ record for the whole core, but failed because the site lies below the calcite compensation depth (CCD). The CCD is located between water depths of 3000 and 3500 m in the study area, although variable positions have been reported (Rottman, 1979; Thunell et al., 1992; Miao et al., 1994; Wang et al., 1995; Wei et al, 1997). Fortunately, foraminifera were obtained for some layers and an age model was developed for the last 9160 cal a BP. Therefore, magnetic properties and its sensitivity to climate change were discussed only for Holocene recorded by the upper 190 cm sediments (95 magnetic samples) in the present paper.

Magnetic Measurements

Grain size and concentration of magnetic minerals of a sample can be identified from magnetic properties (Thompson and Oldfield, 1986; Verosub and Roberts, 1995; Evans and Heller, 2003). A suite of mineral magnetic measurements were made on samples from the studied PC24 sediments. The low-field magnetic susceptibility (χ) was measured for all discrete samples using a Kappabridge MFK1-FA (AGICO) magnetic susceptibility meter at both low (976 Hz) and high (15,616 Hz) frequencies (defined as χ_{lf} *and* χ_{hf}). Frequency-dependent susceptibility χ_{fd}% (reflecting the contribution of superparamagnetic (SP) particles to magnetic susceptibility) was calculated by the equations: $\chi_{fd} = \chi_{lf} - \chi_{hf}$ and $\chi_{fd}\% = 100 \times (\chi_{lf} - \chi_{hf})/\chi_{lf}$ (Evans and Heller, 2003). The temperature dependence of susceptibility (κ-T curves) was measured in an argon atmosphere for nine representative samples from room temperature to 700°C using the Kappabridge MFK1-FA equipped with a CS-4 heating device. These measurements were performed at the Guangzhou Institute of Geochemistry, Chinese Academy of Sciences. All other magnetic measurements were carried out at the Australian National University. An anhysteretic remanent magnetization (*ARM*) was imparted to all samples in a 0.05 mT direct current (DC) bias field with a superimposed 100 mT peak AF. Magnetic susceptibility of ARM was obtained by dividing ARM with the DC bias field. An isothermal remanent magnetization (IRM) was imparted in a 900 mT DC field and a 300 mT backfield, which are treated here as a saturation IRM (*SIRM*) and a IRM_{-300}, respectively a using a 2-G Enterprises 760 pulse magnetizer. *S*-ratios (S_{-300}) were calculated as $S_{-300} = (1\text{-}IRM_{-300\,mT}/SIRM)/2$, following the definition of Bloemendal et al. (1992). Hysteresis loops with a maximum applied field of 0.5 T, IRM acquisition curves with a maximum applied field of 1.0 T, and backfield demagnetization curves were measured for tens of representative samples using a Princeton Measurements Corporation MicroMag^{TM} 3900 vibrating sample magnetometer (VSM). Values of the saturation magnetization (M_s), saturation remanent magnetization (M_{rs}) and coercivity (B_c) were obtained from the hysteresis loops, while the coercivity of remanence (B_{cr}) was determined from the backfield IRM demagnetization curves. Cumulative log-Gaussian (CLG) analyses were completed for all IRM acquisition curves using the IRMUNMIX2_2 and the IRM_CLG1 routines (Kruiver et al., 2001; Heslop et al., 2004).

Elemental Analysis

Twenty bulk samples (10 cm space) were selected for elemental analysis. Concentration of major elements (Al, Ba, Ca, Fe, K, Mg, Mn, Na, Si, and Ti) was measured using the method of X-ray fluorescent spectrum instrument and melting glass. Content of trace elements including rare earth elements was determined by an inductively coupled plasma mass spectrometry using melting method. These elemental analyses were performed at the ALS chemex (Guangzhou) Co., Ltd. Subsamples of ca.

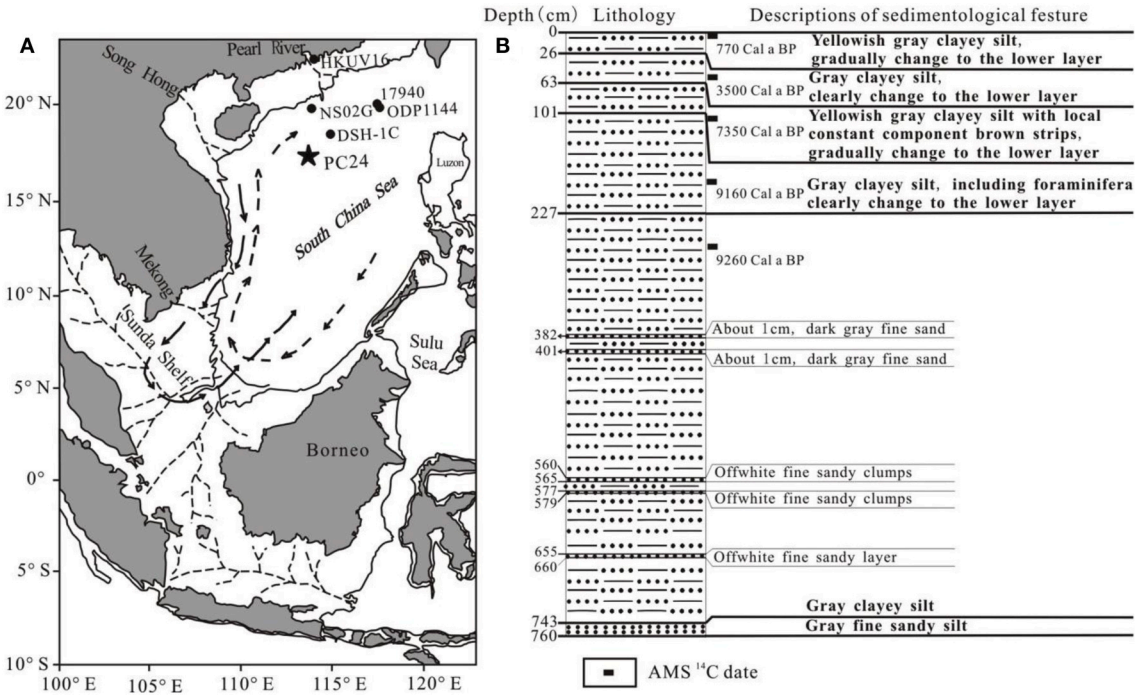

FIGURE 1 | (A) Study area and location of the studied core PC24 and cores for comparison (redrawn from Ouyang et al., 2014a), and **(B)** Sediment lithology of PC24 (redrawn from Ouyang et al., 2014b). The solid and dashed arrows denote surface-water circulation pattern in the SCS during winter and summer, respectively.

0.5 g were digested for 6 h with <10% HCl at room temperature and then heated in a water bath for up to 2 h at 80°C to completely remove carbonate. They were again oven-dried at 80°C after being washed at least 6 times to pH > 6 with distilled water. Sequentially, concentration of total organic carbon (TOC) and $\delta^{13}C_{TOC}$ were measured using an Elementar IsoPrime 100 isotope ratio mass spectrometry (IRMS) instrument interfaced with an Elementar PYRO cube instrument for elemental analysis (EA) at the State Key Laboratory of Isotope Geochemistry, Guangzhou Institute of Geochemistry, Chinese Academy of Sciences.

RESULTS

Age Model

Though the date frame of the whole core need further analysis, the dates upper sediments were accurately given by the results of AMS ^{14}C dating for foraminifera (mainly *Globorotalia menardii* and *Globigerinoides sacculifer*). The radiocarbon ages for upper sediments from the studied core PC24 are given in 1 **Table 1** and **Figure 2**.

The calibrated radiocarbon ages vary nearly linear with depth for the upper 189 cm sediments (**Figure 2A**). However, the ages from the depth 169 to 269 cm rarely increases (**Table 1** and **Figure 2A**). The foraminifera selection results indicated that the total materials for radiocarbon age measurements within the upper 189 cm and the 269 cm sediments were more than 8 mg and less than 3 mg, respectively. Therefore, although the other ages of the upper 189 cm sediments are reasonable, the radiocarbon age of the 269 cm sediments should be much different from its real age and it was incredible. The date for the sediment at depth of 269 cm was ignored during date frame establishment. Sedimentary rate for every stage using the four ages illustrated in **Figure 2B**. Apparently, sedimentary rate differed among different stages and it decreased sharply after 7350 cal. a BP. Therefore, date for each sediment depth was acquired by stepwise calculation using different sedimentary rate and the analyzed AMS ^{14}C results illustrated in **Figure 2B**. The calculated dates of each depth using in the following discussion for upper 0–190 cm sediments are illustrated in **Figure 2B**.

TABLE 1 | The radiocarbon ages for upper sediments of PC24 core.

Depth (cm)	Materials and quantity (mg)	AMS^{14}C (a B.P.)	Cal. Age (a B.P.) (*P* 68%)
1	*Globorotalia menardii* 7.3	845 ± 25	770 ± 30
55	*Globorotalia menardii* 18	3265 ± 30	3500 ± 50
109	*Globorotalia menardii, Globigerinoides sacculifer* 8.1	6405 ± 35	7350 ± 50
189	*Globorotalia menardii* 8.9	8195 ± 35	9160 ± 80
269	*Globorotalia menardii, Globigerinoides sacculifer* 2.7	8265 ± 45	9260 ± 100

All ages were calibrated using the software CalPal. P = probability that the spread of ages is a chance process.

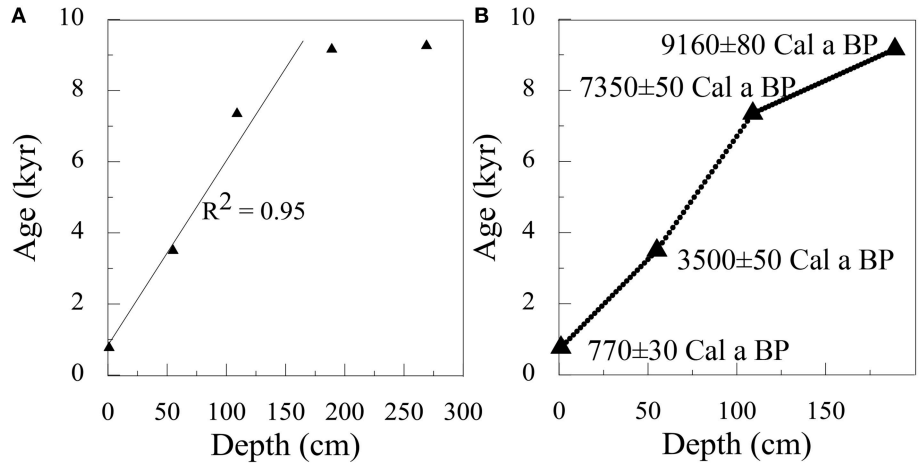

FIGURE 2 | Age-depth models for upper sediments of the studied core (PC24). (A) AMS ^{14}C calibrated ages; **(B)** ages (triangles) using for sedimentary rate and date calculation for every stage and each sediment depth and calculated date of each depth for upper 190 cm sediments.

Magnetic Mineralogy

As the previous published research for the core PC24 (Ouyang et al., 2014a) suggested that both detrital (mainly pseudo single domain, PSD) and biogenic (mainly single domain, SD) magnetite were coexisted within core PC24 sediments. κ-T curves, hysteresis loops, IRM acquisition and backfield demagnetization curves, gradient acquisition plot of IRM acquisition curves from CLG analysis are illustrated at **Figure 3** for representative samples.

κ–T curves for 9 selected samples consistently reveal a major κ decrease at the Curie temperature of magnetite (**Figure 3A**), indicating the presence of magnetite within the studied sediments. For some samples, neoformation of magnetite via conversion of Fe-clay minerals is evident during heating (Deng et al., 2004; Zhang et al., 2012), which causes κ to increase above 300°C up to just below the Curie temperature of magnetite. The much higher κ values during cooling processes prove the production of new magnetite (**Figure 3A**). Some single domain (SD) magnetite particles are proved to be present within some samples by Hopkinson peaks in the heating curves (**Figure 3A**) (Dunlop and Özdemir, 2015). Hysteresis loops before and after paramagnetic slope correction (**Figure 3B**) indicated that paramagnetic components and low coercivity spectra were determined. According to the results of Hysteresis loops, IRM acquisition curves and B_{cr} values, low coercivity magnetic minerals were predominated the studied sediments (**Figures 3B,C**). Two low coercivity magnetic components were identified from the CLG analysis of IRM acquisition curves (**Figure 3D**) (Kruiver et al., 2001). For the analyzed samples, average contributions to the IRM of the two components are 50.3 and 49.6%, with average $B_{1/2}$ of 30.5 mT and 40.8 mT, respectively. These results indicate that the two magnetic components are magnetite with different grain sizes.

Mean B_{cr}/B_c and M_{rs}/M_s values for 20 analyzed samples are 2.33 and 0.25, respectively. As discussed within the previous article (Ouyang et al., 2014a), granularity of magnetic minerals reflected by Day-plot, King-plot and FORC diagrams suggested both detrital pseudo-single domain (PSD) and biogenic single domain (SD) magnetite particles (DM and BM, respectively) were concurrence within the studied sediments. As shown in the previous published article (Ouyang et al., 2014a), both non-interacting biogenic magnetite and a detrital magnetite were identified from the FORC diagrams (not shown here) of all sediments from the whole core PC24.

Vertical Variation of Magnetic Properties

The concentration dependent parameters χ, χ_{ARM}, and SIRM appeared basically consistent variation trends (**Figures 4A–C**). Total content of magnetite reflected by these parameters remained relatively stable during 9.16–7.4 cal. ka BP, and increased to a high level following with a sharp decrease at 3.4 cal. ka BP. After experiencing a decreasing trend, they increased gradually after 2.7 cal. ka BP. Although content of different origin magnetite can't be calculated exactly, content of detrital and biogenic magnetite reflected by IRM_DM and IRM_BM varied reversely during 6.8–3.9 cal. ka BP (**Figures 4H,I**).

The value of the *S*-ratio can reflect the relative amounts of high versus low coercivity magnetic minerals (Thompson and Oldfield, 1986; Verosub and Roberts, 1995; Evans and Heller, 2003). It is close to 1.0 for pure ferromagnetic samples, and decreases with increasing contribution of antiferromagnetic minerals. The pre-mentioned magnetic mineralogy results indicated that two components of magnetite with different grain size were coexisted within the studied sediments. As a result, the S_{-300} values of the studies sediment core were close to 1.0 (varied between 0.94 and 0.98, **Figure 4D**). Variation of S_{-300} may reflect the relative contribution of DM and BM to total magnetics.

Generally, variation of grain size dependent indicators $\chi_{ARM}/SIRM$ and $SIRM/\chi$ was consistent in sediment cores. However, these two parameters varied oppositely within our studied sediment core (**Figures 4F,G**). During early and middle Holocene, both $\chi_{ARM}/SIRM$ and $SIRM/\chi$ kept relatively stable.

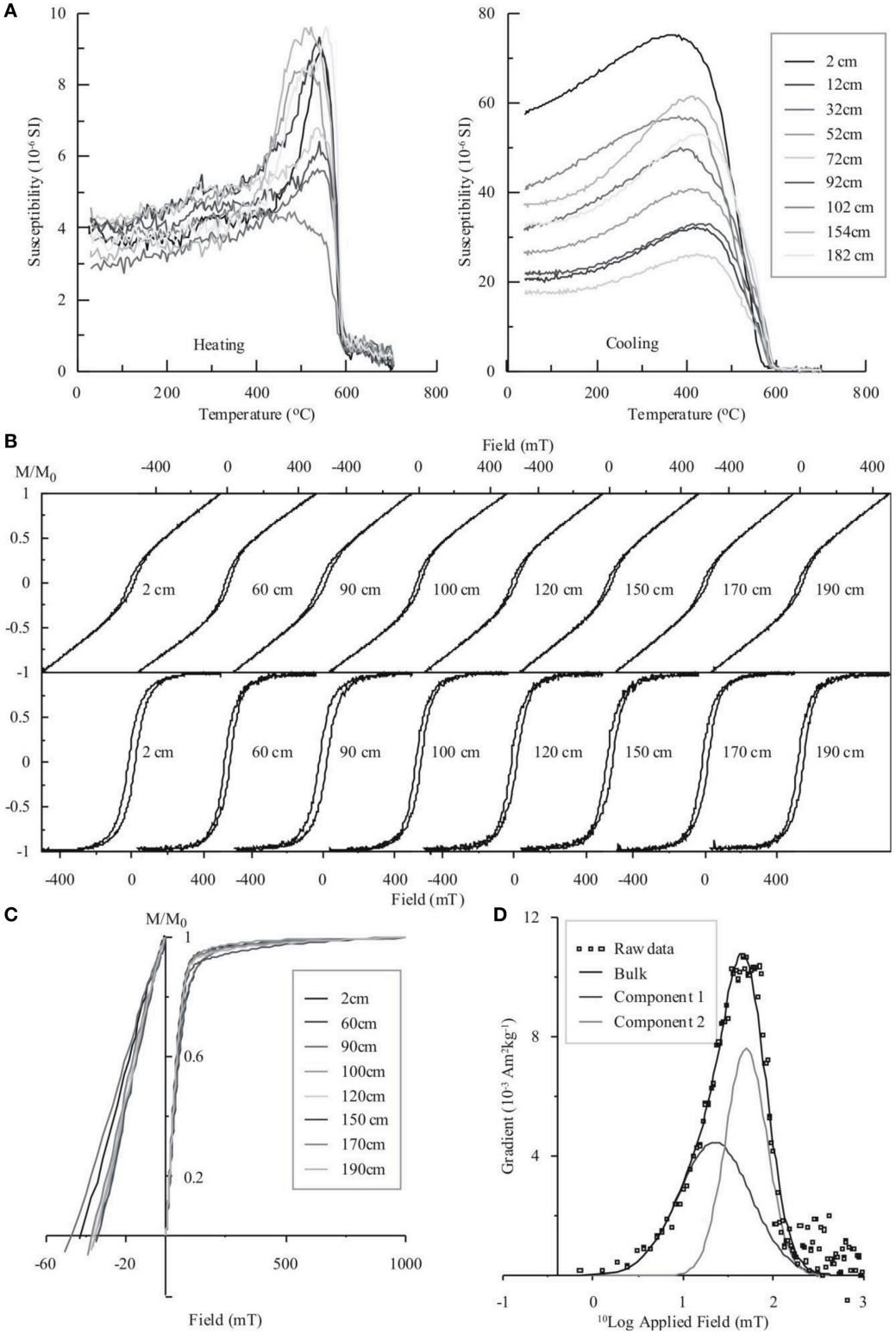

FIGURE 3 | Mineral magnetic properties for sediments from core PC24. Representative **(A)** κ-T curves, **(B)** hysteresis loops before and after paramagnetic slope correction, **(C)** IRM acquisition and backfield demagnetization curves, and **(D)** gradient acquisition plot (GAP) of IRM acquisition curves. The GAP is decomposed into 2 components due to detrital (magnetically softer, wide dispersion; component 1) and biogenic (magnetically harder, narrow dispersion; component 2) magnetite.

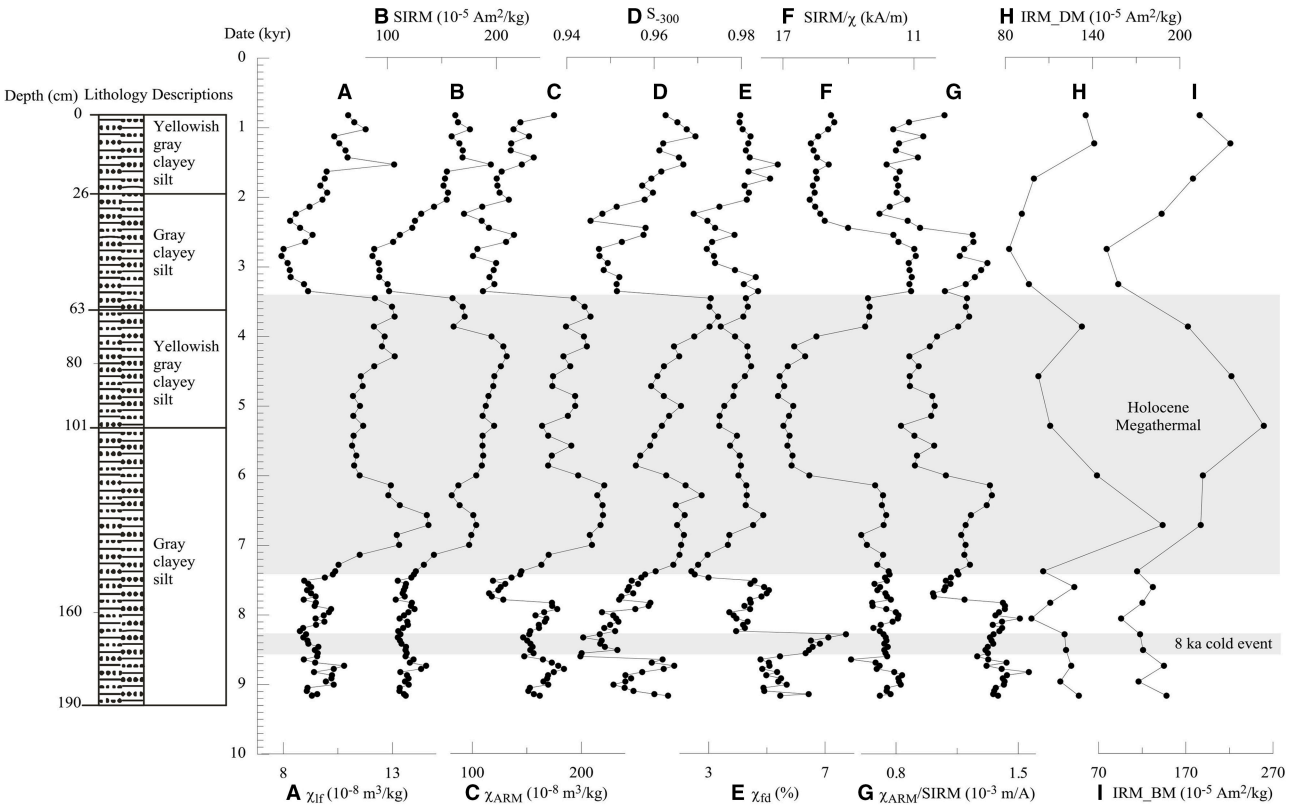

FIGURE 4 | Stratigraphic variations of magnetic parameters. IRM_DM and IRM_BM present IRM carried by detrital and biogenic magnetite, respectively. The shaded areas represent the 8 ka cold event and the Holocene Megathermal, respectively.

SIRM/χ increased sharply since 6.1 cal. ka BP and decreased to the lowest value at 3.4 cal. ka BP. High and low values of SIRM/χ and χ_{ARM}/SIRM were appeared after 2.7 cal. ka BP, respectively.

DISCUSSION

Origin of Magnetic Particles

As pre-mentioned by coercivity distribution, both detrital (PSD) and biogenic (SD) magnetite were concurrence within the studied sediments (**Figure 3D**). Scatter plot between χ_{lf} and χ_{ARM} illustrated within **Figure 7B** indicated that biogenic SD magnetite particles within the studied sediments played important contribution to χ of the studied sediments. The significant positive correlation between χ_{lf} and SIRM (**Figure 7B**) indicated that the variation of these two parameters was largely controlled by a common effect of type and concentration of magnetic minerals. Differed from many previous studies (Yu and Oldfield, 1989; Ouyang et al., 2013), no obvious correlation was appeared between χ_{lf} and χ_{fd}% (**Figure 7A**), indicating that superparamagnetic (SP) particles were not the main controller for magnetic susceptibility. However, some superparamagnetic (SP) magnetite particles might be also appeared within the studied sediments due to relatively high average value of χ_{fd} (average 4.54×10^{-9} m^3/kg) and significant paramagnetic signals during hysteresis measurements (**Figure 3B**).

Many sources can bring the mentioned SP, PSD, and SD magnetic particles to marine sediments. However, magnetic minerals from different sources can play significant and different potential impact on sediment magnetic properties. Hilton (1987) pointed that eolian deposition and magnetic bacteria might be important in deep-ocean sediments. According to the results of provenance analysis for the study area, besides sediments carried by ocean current, some fluvial alluvial sediments as well as eolian dust can also be deposited at the station of the study core. Weathering materials around the study area can be transported by runoff to deposit in the sampling station. Meanwhile, eolian dusts as well as fly ash can be transported by wind to the waters (Liu et al., 2007, 2008, 2010; Wei et al., 2012). Therefore, the PSD and SP detrital magnetite should be from river input and north Asian eolian particles. In addition, eolian particles and river input might mainly contribute to SP and PSD magnetic particles, respectively. As suggested by the previous published article of the studied core, the biogenic SD magnetite particles should be from marine authigenesis or post-deposition bacterial action.

Dypvik and Harris (2001) pointed out that Th/U ratio was sensitive to redox condition. Th/U ratio below one indicated reducing conditions. The high values of this ratio (4.14–6.55) for

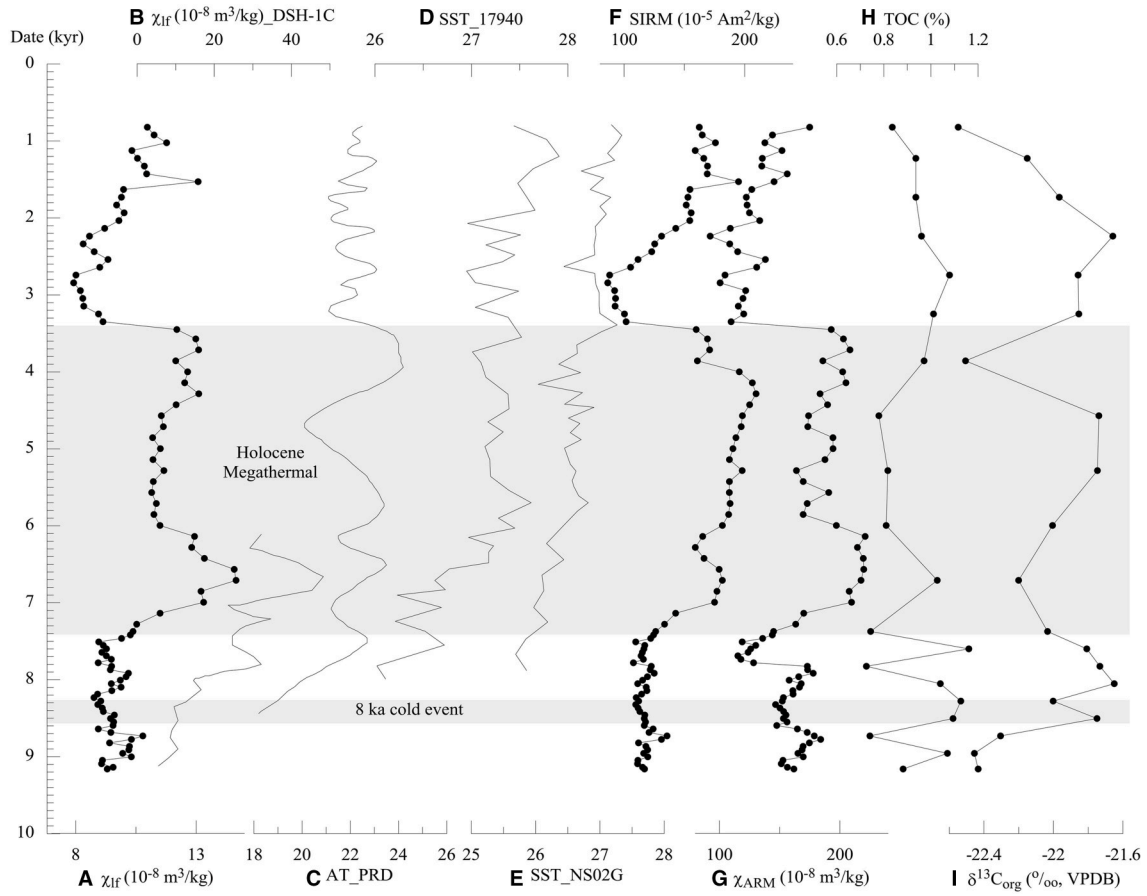

FIGURE 5 | Variation of concentration dependent magnetic parameters and TOC contents and $\delta^{13}C_{org}$ of the studied core PC24 compared with the low-field magnetic susceptibility of core DSH-1C (Luo et al., 2010), air temperature (AT) of the Pearl River Delta (PRD) (Fang et al., 1991), sea surface temperature (SST) of core NS02G (Kong et al., 2014) and core 17940 (Wang et al., 1999).

the studied PC24 sediments indicated an oxidative deposition condition. Moreover, the relatively low value of SIRM/κ (10.9–17.2 kA/m) showed that no iron sulfide was present within the sediments and the influence of early reductive diagenesis on the sediments was very limited.

Sensitive Magnetic Parameters to Climatic Variation

Although concentration dependent magnetic parameters χ_{lf}, χ_{ARM} and *SIRM* were sensitive to different grain size magnetic particles, a significant positive correlation was appeared among these parameters (**Figure 7B**). This correlation implies that total content of all magnetic particles is affected by a common factor. Total concentration of magnetic minerals within marine sediments was proved to be related to variation of temperature despite that sediment magnetic response to climate change differed from different regions within the SCS (Hou et al., 1996; Tang et al., 2003; Zhang et al., 2010; Ouyang et al., 2014a). Variation of χ_{lf}, χ_{ARM} and *SIRM* for the studied core PC24 was coincident with variation of χ_{lf} for a previous reported core DSH-1C from the northern SCS before 6 cal. ka B.P (**Figure 5B**) (Luo et al., 2010). Generally, temperature can play important impact on sea level, weathering intension, and marine authigenesis (Chen et al., 2000). Though variation of TOC and $\delta^{13}C_{org}$ was not exactly same to concentration dependent magnetic parameters, the changing trends of these proxies were consistent. Furthermore, a significant positive correlation was appeared between Al/Ti ratio, which can reflect weathering intensity of source area (Zhao and Yan, 1994; Huang et al., 2016), and concentration dependent magnetic parameter SIRM (**Figure 8A**). In addition, χ_{lf}, χ_{ARM} and *SIRM* showed consistent variation trends with air temperature (AT) of the Pearl River Delta (PRD) (Fang et al., 1991), sea surface temperature (SST) of core NS02G (Kong et al., 2014) and core 17940 (Wang et al., 1999) during most stages (**Figure 5**). Therefore, concentration dependent magnetic parameters χ_{lf}, χ_{ARM} and *SIRM* of the studied sediments might have a positive response to variation of temperature.

PSD and SP magnetite particles might be related to river runoff/precipitation and wind speed/dryness, respectively due to their sources and transportation dynamics. Previous research

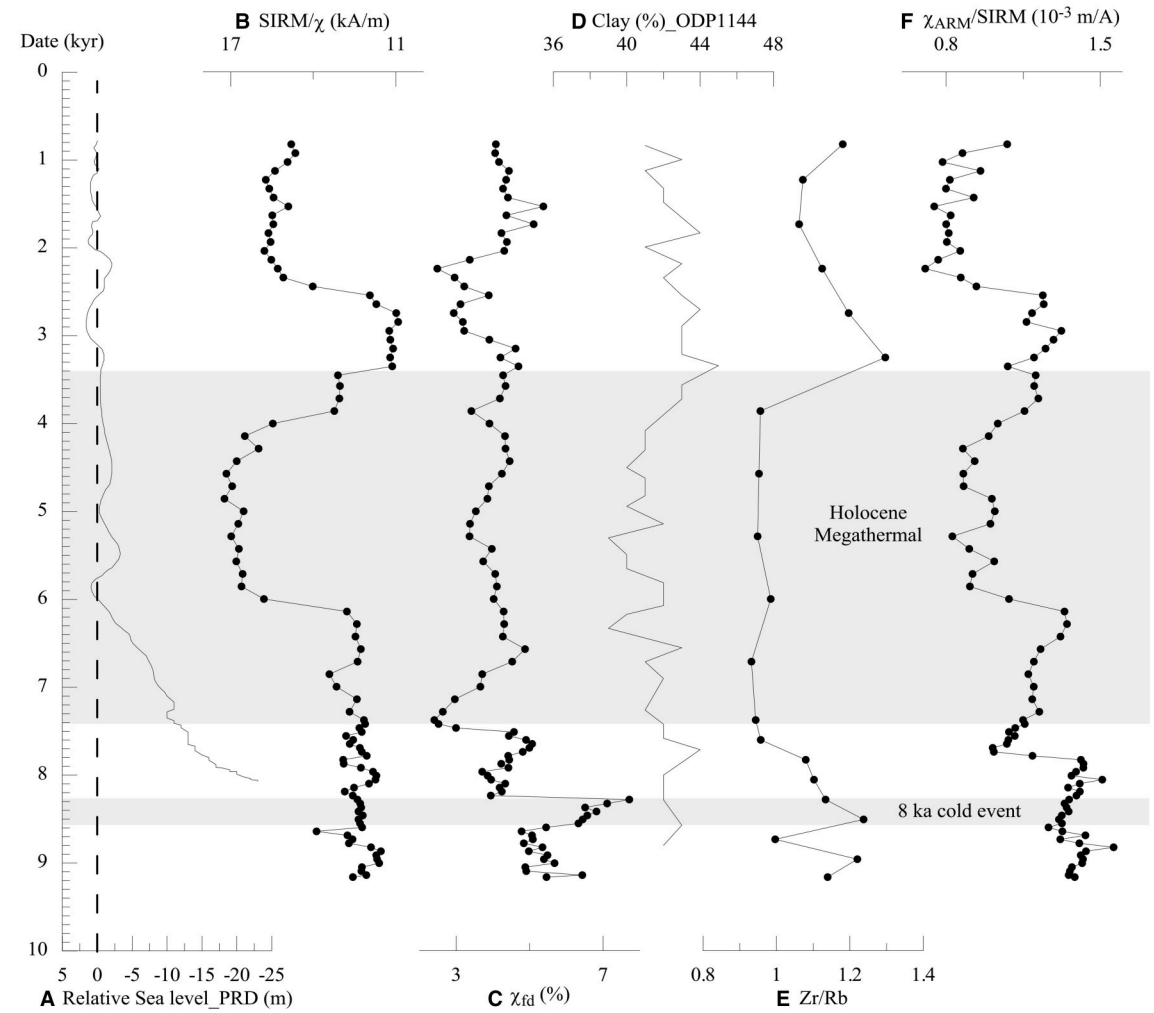

FIGURE 6 | Variation of grain size dependent magnetic parameters and Zr/Rb ratio of PC24 compare with relative sea level of the PRD (Fang et al., 1991) and clay (%) of ODP 1144 (Hu et al., 2012).

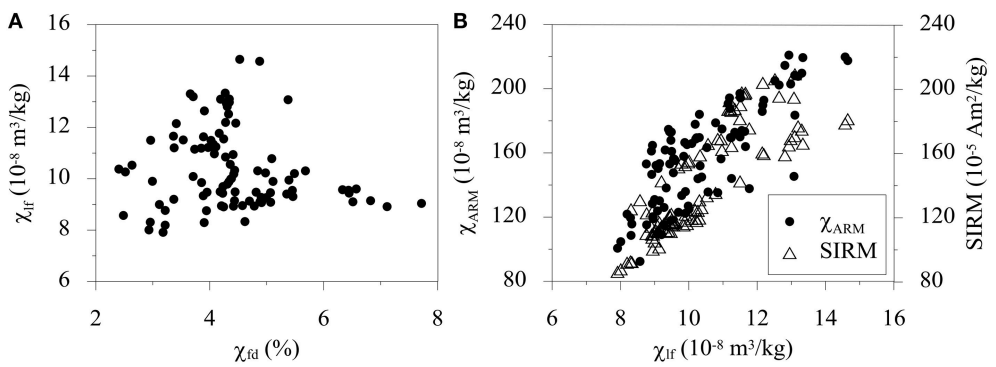

FIGURE 7 | Scatter plot among magnetic parameters. (A) χ_{lf} versus χ_{fd} (%); **(B)** Relationship between χ_{lf} and χ_{ARM}, and between χ_{lf} and SIRM.

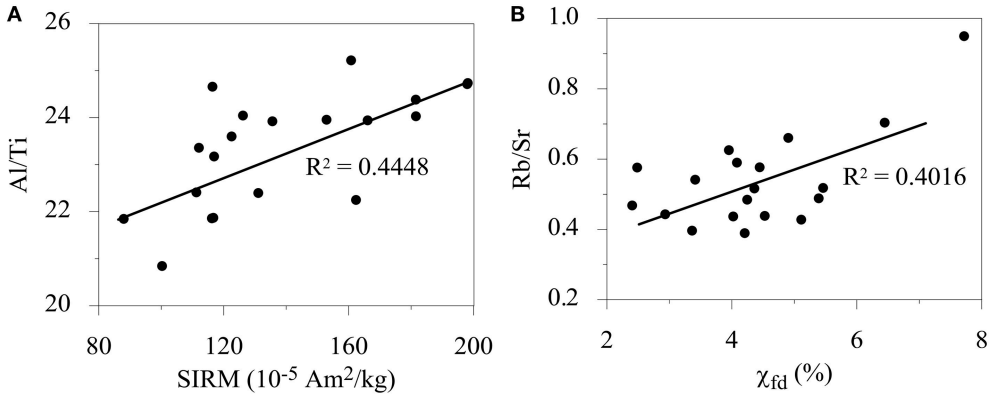

FIGURE 8 | Correlation of (A) Al/Ti and SIRM, (B) Rb/Sr and χ_{fd} (%).

suggested that variation of Zr and Rb within sediments was controlled by unitary factor (Wronkiewicz and Condie, 1987). Furthermore, Dypvik and Harris (2001) pointed out that Zr/Rb ratio of sediments might reflect the strength of wind carrying. The consistent changing trends of χ_{fd} (%), Zr/Rb ratio of the studied core PC24 and clay % of core ODP 1144 indicated that χ_{fd} (%) should correspond to windy intensity. As Wang (1989) pointed, Rb/Sr ratio of marine sediments can reflect the quantity of eolian dust input. High Rb/Sr reflects intense weathering of source and high eolian dust input (Huang et al., 2007; Wang et al., 2012; Luo et al., 2015). High χ_{fd} (%) reflects high contribution of SP particles to magnetic susceptibility (Thompson and Oldfield, 1986; Verosub and Roberts, 1995; Evans and Heller, 2003). The significant positive correlation between these two parameters (**Figure 8B**) indicated intense weathering dust varied simultaneously with SP magnetic particles within sediments (Zan et al., 2015). According to the transportation of dust, more dust deposition within marine sediments must be due to windy and dry climate. Therefore, χ_{fd} (%) of the studied sediments should be related to humidity of the study area. Higher Rb/Sr ratio and χ_{fd} (%) is corresponded to drier climate.

As pre-mentioned, χ_{ARM}/*SIRM* varied reversely to *SIRM*/χ. Moreover, correlation analysis results indicated that a significant negative correlation was appeared between these two parameters for the studied sediments ($R^2 = 0.60$). These results should be caused by the different relative contributions of the two components of magnetite during different periods. Comparing to the contribution of the two magnetite components to *SIRM*, contribution of DM and BM to SIRM was significant positive related to χ_{ARM}/*SIRM* and *SIRM*/χ (**Figure 9**), respectively. Therefore, it can be speculated that χ_{ARM}/*SIRM* was sensitive to detrital magnetite particles and *SIRM*/χ was effective to biogenic magnetite particles. Since SP particles do not carry any magnetic remanence, χ_{ARM}/*SIRM* is specifically reflected the detrital PSD magnetic particles. Coarser particles can be transported into the study area within more humid climate due to higher runoff. Moreover, χ_{ARM}/*SIRM* consistently varied with Zr/Rb ratio, χ_{fd} (%) and clay % of core ODP 1144 (**Figure 6**). Therefore, variation of χ_{ARM}/*SIRM* should be consistent with dryness of the study area. As pre-mentioned, biogenic magnetite particles should be from marine authigenesis or post-deposition bacterial action. The basically consistent trends of *SIRM*/χ and relative sea level of the PRD (Fang et al., 1991) indicated that *SIRM*/χ might be corresponding to temperature which is related to seal level (**Figure 6**).

Summarily, climatic sensitive magnetic parameters include concentration and grain size dependent indicators. High values of χ_{fd} (%) and χ_{ARM}/*SIRM* correspond to dry climate. Furthermore, χ_{ARM}/*SIRM* should be more effective due to relatively low concentration of SP magnetic particles within the studied sediments. On the other hand, high values of concentration dependent magnetic parameters χ_{lf}, χ_{ARM} and *SIRM* as well as *SIRM*/χ might reflect warm climate. On the contrary, low values of these parameters indicate wet or cool climate.

Climate Change During Holocene Recorded by Magnetic Properties

Generally, climate combinations are warm wet and cold dry at most regions. However, the magnetic results indicated that the climate combinations were warm dry and cold wet in the study area during early and middle Holocene. This decoupling of temperature and precipitation has been reported for the area from south China to the SCS (Yokoyama et al., 2011; Zhang et al., 2015). During 9.16–7.8 cal. ka BP, the concentration dependent magnetic parameters as well as χ_{ARM}/*SIRM* and *SIRM*/χ kept relatively stable (**Figure 4**), indicating a relatively stable climate (including temperature and precipitation) during this period. The climate fluctuated frequently since 7.8 cal. ka BP. The Holocene climate fluctuations reflected by magnetic properties of PC24 sediments were basically consistent to the results of Shi et al. (1992). However, climate change recorded by magnetic properties of PC24 differed slightly from their results. According to Shi et al. (1992), the period during 8.5–3.0 ka BP was identified as the Holocene Megathermal, the latest Hysithermal,

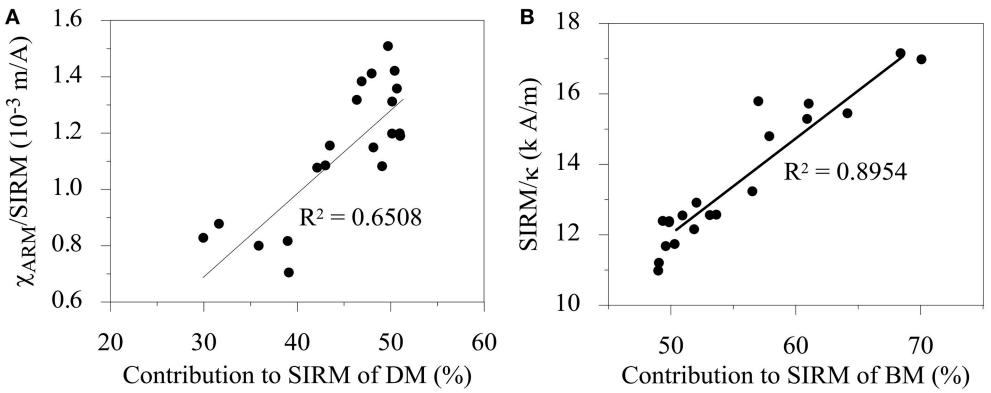

FIGURE 9 | Correlation between grain size dependent magnetic parameter and contribution of magnetic components to SIRM. (A) Contribution of detrital magnetite to SIRM and χ_{ARM}/SIRM; **(B)** Contribution of biogenic magnetite to SIRM and SIRM/χ.

inland of China. However, the magnetic properties of core PC24 sediments indicated that the beginning and duration of the Holocene Megathermal for the study area were different. The values of concentration dependent magnetic parameters increased gradually from 7.5 cal. ka BP. The increasing χ_{fd} (%) from 7.5 cal. ka BP indicates climate grows drier. Increasing eolian dust input but low marine authigenesis should explain the highest values of χ_{lf}, χ_{ARM} and *SIRM* with relatively low value of during 7.35–6.00 cal. ka BP. *SIRM*/χ reached its peak value during 6.1–3.9 cal. ka BP. Therefore, it seemed that the Holocene Megathermal in the study area of core PC24 was more appropriate during 7.5–3.4 cal. ka BP. This different duration of Holocene Megathermal might be significant for climate response because the same methods (AMS ^{14}C) and low error (less than 100 years) of age determination used by previous research and the present study. This difference indicated that marine response to climate change was slower than inland. The duration 6.1–3.9 cal. ka BP should be identified as the Megathemal Maximum for the study area. The relatively low values of χ_{ARM}/*SIRM* during the warmest stage of Holocene reveal a relative wet condition during this period. χ_{lf}, χ_{ARM}, *SIRM*, and *SIRM*/χ decreased sharply from 3.4 cal. ka BP, indicating the climate got cool abruptly. Since 2.7 cal. ka BP, χ_{lf}, χ_{ARM}, *SIRM*, and *SIRM*/χ increased and χ_{ARM}/*SIRM* decreased gradually, indicating the climate became warm and wet.

According to Jin et al. (2007), it should be open to discussion whether there was a synchronous or similar event or not as the worldwide recorded 8.2 ka cooling event in China. However, the results indicated that a similar cold event as 8.2 ka cooling event was also recorded by magnetic properties of core PC24 sediments. From 8.55 to 8.25 cal. ka BP., values of χ_{lf}, χ_{ARM}, *SIRM*, and *SIRM*/χ decreased slightly. Value of χ_{fd} (%) rose greatly and reached its highest value. These results indicated that the local climate of core PC24 during this stage was manifested as cold dry.

CONCLUSIONS

Approximately equal concentration of detrital PSD and biogenic SD magnetite and small part of SP particles were coexisted within the studied core (PC24) sediments. The concentration dependent magnetic parameters are positive corresponding to variation of temperature. Grain size dependent parameters χ_{ARM}/*SIRM* and *SIRM*/χ of the studied core sediments varied reversely. Comparing to the contribution of detrital PSD and biogenic SD magnetite to SIRM, it can be deduced that magnetic parameters χ_{ARM}/*SIRM* and *SIRM*/χ are sensitive to detrital and biogenic magnetite particles, respectively. Variations of χ_{ARM}/*SIRM* and *SIRM*/χ are corresponding to humidity and temperature, respectively.

The local climate of the study area fluctuated during Holocene. During early and middle Holocene, the climate combinations were warm dry and cold wet. It became warm and wet since 2.7 cal. ka BP. The Holocene Megathermal in the study area recorded by magnetic properties of core PC24 was appropriate during 7.5–3.4 cal. ka BP. The warmest stage of Holocene for the study area should be during 6.1–3.9 cal. ka BP. The cold event at 8 ka was characterized as cold and dry during 8.55–8.25 cal. ka BP.

AUTHOR CONTRIBUTIONS

All authors listed, have made substantial, direct and intellectual contribution to the work, and approved it for publication.

ACKNOWLEDGMENTS

This work was partially supported by the National Science Foundation of China (grant 41272384), the National Basic Research Project (grant 2010CB833405) and a grant from Youth Innovation Promotion Association of the Chinese Academy of Sciences (grant 2012262). The authors thank Luhua Xie for his help during TOC and $\delta^{13}C_{org}$ measurements.

REFERENCES

Arai, K., Sakai, H., and Konishi, K. (1997). High-resolution rock-magnetic variability in shallow marine sediment: a sensitive paleoclimatic metronome. *Sediment. Geol.* 110, 7–23. doi: 10.1016/S0037-0738(96)00082-6

Bloemendal, J., King, J. W., Hall, F. R., and Doh, S. J. (1992). Rock magnetism of late Neogene and Pleistocene deep-sea sediments: relationship to sediment source, diagenetic processes, and sediment lithology. *J. Geophys. Res.* 97, 4361–4375. doi: 10.1029/91JB03068

Chen, M. H., Wang, R. J., Yang, L. H., Han, J. X., and Lu, J. (2003). Development of east Asian summer monsoon environments in the late Miocene: radiolarian evidence from site 1143 of ODP Leg 184. *Mar. Geol.* 201, 169–177. doi: 10.1016/S0025-3227(03)00215-9

Chen, M., Tu, X., and Zhang, F. (2000). Relations between sedimentary sequence and paleoclimatic changes during last 200 ka in the southern South China Sea. *Chinese Sci. Bull.* 45, 1334–1340. doi: 10.1007/BF03182915

Deng, C. L., Zhu, R. X., Verosub, K. L., Singer, M. J., and Vidic, N. J. (2004). Mineral magnetic properties of loess/paleosol couplets of the central loess plateau of China over the last 1.2 Myr. *J. Geophys. Res.* 109, B01103. doi: 10.1029/2003jb002532

Dunlop, D. J., and Özdemir, Ö. (2015). "Magnetizations in rocks and minerals," in *Treatise on Geophysics, 2nd Edn.*, ed S. Gerald (Elsevier), 255–308. doi: 10.1016/B978-0-444-53802-4.00102-0

Dypvik, H., and Harris, N. B. (2001). Geochemical facies analysis of fine-grained siliciclastics using Thu/U, Zr/Rb and (Zr+Rb)/Sr ratios. *Chem. Geol.* 181, 131–146. doi: 10.1016/S0009-2541(01)00278-9

Evans, M. E., and Heller, F. (2003). *Environmental Magnetism: Principles and Applications of Enviromagnetics*. San Diego, CA: Acdemic Press.

Fang, G. X., Li, P. R., and Huang, G. Q. (1991). Sea level changes in Zhujiang Delta during the past 8000 years. *Geogr. Res.* 10, 1–11 (in Chinese with English abstract).

Han, J. T., and Fyfe, W. S. (1995). Ocean response to the last deglaciation: conventional paleoclimate models and controversy. *Quatern. Sci.* 1, 89–95 (in Chinese with English abstract).

He, L. S., and Chen, B. Y. (1987). *The Tectonic Map, The South China Sea Geological and Geophysical Atlas*. Guangzhou: Guangdong Cartographic Press.

Heslop, D., McIntosh, G., and Dekkers, M. J. (2004). Using time- and temperature-dependent Preisach models to investigate the limitations of modeling isothermal remanent magnetization acquisition curves with cumulative log Gaussian functions. *Geophys. J. Int.* 157, 55–63. doi: 10.1111/j.1365-246X.2004.02155.x

Heslop, D., and Roberts, A. P. (2013). Calculating uncertainties on predictions of palaeoprecipitation from the magnetic properties of soils. *Glob. Planet Change* 110, 379–385. doi: 10.1016/j.gloplacha.2012.11.013

Hilton, J. (1987). A simple model for the interpretation of magnetic records in lacustrine and ocean sediments. *Q. Res.* 27, 160–166. doi: 10.1016/0033-5894(87)90074-3

Hou, H. M., Wang, B. G., and Tang, X. Z. (1996). A response to paleoclimatic nonlinear variations from sediment magnetic susceptibility in northern South China Sea. *Tropic Oceanol.* 15, 1–5 (in Chinese with English abstract).

Hu, D. K., Böning, P., Köhler, C. M., Hillier, S., Pessling, N., Wang, S. M., et al. (2012). Deep sea records of the continental weathering and erosion response to East Asian monsoon intensification since 14 ka in the South China Sea. *Chem. Geol.* 326–327, 1–18. doi: 10.1016/j.chemgeo.2012.07.024

Huang, J., Wan, S. M., Xiong, Z. F., Zhao, D. B., Liu, X. T., Li, A. C., et al. (2016). Geochemical records of Taiwan-sourced sediments in the South China Sea linked to Holocene climate changes. *Palaeogeogr. Palaeoclimatol. Palaeoecol.* 441, 871–881. doi: 10.1016/j.palaeo.2015.10.036

Huang, R., Zhu, C., and Wang, S. T. (2007). Magnetic susceptibility and Rb/Sr Ratio of peat stratum in tiantangzhai and its significance of palaeoclimate. *Sci. Geogr. Sinica* 27, 385–389 (in Chinese with English abstract).

Jin, H. Y., and Jian, Z. M. (2008). Comparison of climate changes between northern and southern South China Sea during the mid-Pleistocene climate transition period. *Quatern. Sci.* 28, 381–390 (in Chinese with English abstract).

Jin, Z. D., Yu, J. M., Wu, Y. H., and Wang, S. M. (2007). Was there an 8.2 ka BP cooling event in China? *Geol. Rev.* 53, 616–623 (in Chinese with English abstract).

Kissel, C., Laj, C., Clemens, S., and Solheid, P. (2003). Magnetic signature of environmental changes in the last 1.2 Myr at ODP Site 1146, South China Sea. *Mar. Geol.* 201, 119–132. doi: 10.1016/S0025-3227(03)00212-3

Kissel, C., Laj, C., Labeyrie, L., Dokken, T., Voelker, A., and Blamart, D. (1999). Rapid climatic variations during marine isotopic stage 3: magnetic analysis of sediments from Nordic Seas and North Atlantic. *Earth Planet. Sci. Lett.* 171, 489–502. doi: 10.1016/S0012-821X(99)00162-4

Kong, D. M., Zong, Y. Q., Jia, G. D., Wei, G. J., Chen, M. T., and Liu, Z. H. (2014). The development of late Holocene coastal cooling in the northern South China Sea. *Quatern. Int.* 349, 300–307. doi: 10.1016/j.quaint.2013.08.055

Kruiver, P. P., Dekkers, M. J., and Heslop, D. (2001). Quantification of magnetic coercivity components by the analysis of acquisition curves of isothermal remanent magnetization. *Earth Planet. Sci. Lett.* 189, 269–276. doi: 10.1016/S0012-821X(01)00367-3

Kumar, A. A., Purnachandra, V., Patil, S. K., Kessarkar, M., and Thamban, M. (2005). Rock magnetic records of the sediments of the eastern Arabian Sea: evidence for late quaternary climatic change. *Mar. Geol.* 220, 59–82. doi: 10.1016/j.margeo.2005.06.038

Larrasoaña, J. C., Roberts, A. P., Liu, Q., Lyons, R., Oldfield, F., Rohling, E. J., et al. (2015). Source-to-sink magnetic properties of NE Saharan dust in Eastern Mediterranean marine sediments: review and paleoenvironmental implications. *Front. Earth Sci.* 3:19. doi: 10.3389/feart.2015.00019

Liu, G. D. (ed.). (1992). *The Geological and Geophysical Map of the China's Seas and Adjacent Areas* (at scale of 1:5 million). Beijing: Geological Publishing House.

Liu, J. G., Chen, Z., Chen, M. H., Yan, W., Xiang, R., and Tang, X. Z. (2010). Magnetic susceptibility variations and provenance of surface sediments in the South China Sea. *Sediment. Geol.* 230, 77–85. doi: 10.1016/j.sedgeo.2010.07.001

Liu, Z. F., Colin, C., Huang, W., Chen, Z., Trentesaux, A., and Chen, J. F. (2007). Clay minerals in surface sediments of the Pearl River drainage basin and their contribution to the South China Sea. *Chinese Sci. Bull.* 52, 1101–1111. doi: 10.1007/s11434-007-0161-9

Liu, Z. F., Tuo, S. T., Colin, C., Liu, J. T., Huang, C. Y., Selvaraj, K., et al. (2008). Detrital fine-grained sediment contribution from Taiwan to the northern South China Sea and its relation to regional ocean circulation. *Mar. Geol.* 255, 149–155. doi: 10.1016/j.margeo.2008.08.003

Luo, Q. Y., Zhong, N. N., Wang, Y. N., Ma, L., and Li, M. (2015). Provenance and paleoweathering reconstruction of the Mesoproterozoic Hongshuizhuang Formation (1.4 Ga), northern North China. *Int. J. Earth Sci.* 104, 1701–1720. doi: 10.1007/s00531-015-1163-5

Luo, Y., Su, X., Chen, F., and Huang, Y. Y. (2010). Magnetic properties of late Pleistocene sediments in core DSH-1C from northern South China Sea and their environment significance. *Geoscience* 24, 521–527 (in Chinese with English abstract).

Maher, B. A. (2007). Environmental magnetism and climate change. *Contemp. Phys.* 48, 247–274. doi: 10.1080/00107510801889726

Miao, Q. M., Thunell, R. C., and Anderson, D. M. (1994). Glacial-Holocene carbonate dissolution and sea surface temperatures in the South China and Sulu Seas. *Paleoceanography* 9, 269–290. doi: 10.1029/93PA02830

Moreno, E., Thouveny, N., Delanghe, D., McCave, I. N., and Shackleton, N. J. (2002). Climatic and oceanographic changes in the Northeast Atlantic reflected by magnetic properties of sediments deposited on the Portuguese Margin during the last 340 ka. *Earth Planet Sci. Lett.* 202, 465–480. doi: 10.1016/S0012-821X(02)00787-2

Oldfield, F., Asioli, A., Accorsi, C. A., Mercuri, A. M., Juggins, S., Langone, L., et al. (2003). A high resolution late Holocene palaeo environmental record from the central Adriatic Sea. *Quaternary Sci. Rev.* 22, 319–342. doi: 10.1016/S0277-3791(02)00088-4

Ouyang, T. P., Appel, E., Jia, G. D., Huang, N. S., and Zhu, Z. Y. (2013). Magnetic mineralogy and its implication of contemporary coastal sediments from South China. *Environ. Earth Sci.* 68, 1609–1617. doi: 10.1007/s12665-012-1854-1

Ouyang, T. P., Heslop, D., Roberts, A. P., Tian, C. J., Zhu, Z. Y., Qiu, Y., et al. (2014b). Variable remanence acquisition efficiency in sediments containing biogenic and detrital magnetites: implications for relative paleointensity signal recording. *Geochem. Geophys. Geosyst.* 15, 2780–2796. doi: 10.1002/2014GC005301

Ouyang, T. P., Tian, C. J., Zhu, Z. Y., Qiu, Y., Appel, E., and Fu, S. Q. (2014a). Magnetic characteristics and its environmental implications of core YSGD-86GC sediments from the southern South China Sea. *Chinese Sci. Bul.* 59, 3176–3187. doi: 10.1007/s11434-014-0438-8

Rottman, M. L. (1979). Dissolution of planktonic *foraminifera* and pteropods in the South China Sea sediments. *J. Foraminiferal Res.* 9, 41–49. doi: 10.2113/gsjfr.9.1.41

Sangode, S. J., Sinha, R., Phartiyal, B., Chauhan, O. S., Mazari, R. K., Bagati, T. N., et al. (2007). Environmental magnetic studies on some quaternary sediments of varied depositions settings in the Indian sub-continent. *Quatern. Int.* 159, 102–118. doi: 10.1016/j.quaint.2006.08.015

Shi, Y. F., Kong, Z. C., Wang, S. M., Tang, L. Y., Wang, F. B., Yao, T. D., et al. (1992). Climate fluctuations and important events during the Holocene Megathermal in China. *China Sci.* 12, 1300–1308 (in Chinese).

Tang, X. Z., Chen, Z., Yan, W., and Chen, M. H. (2003). Youger Dryas and Heinrich events recorded by magnetic susceptibility of sediments from the central temperature area of western Pacific warm pool. *Chinese Sci. Bull.* 48, 491–495. doi: 10.1007/bf03187058

Thompson, R., and Oldfield, F. (1986). *Environmental Magnetism*. *London: Allen & Imwin.*

Thunell, R. C., Miao, Q. M., Calvert, S. E., and Pedersen, T. F. (1992). Glacial-Holocene biogenic sedimentation patterns in the South China Sea: productivity variations and surface water pCO_2. *Paleoceanography* 7, 143–162. doi: 10.1029/92PA00278

Verosub, K. L., and Roberts, A. P. (1995). Environmental magnetism: past, present, and future. *J. Geophys. Res.* 100, 2175–2192. doi: 10.1029/94JB02713

Wan, S. M., Li, A. C., Clift, P. D., and Stuut, J. B. W. (2007). Development of the East Asian monsoon: mineralogical and sedimentologic records in the northern South China Sea since 20 Ma. *Palaeogeogr. Palaeoclimatol. Palaeoecol.* 254, 561–582. doi: 10.1016/j.palaeo.2007.07.009

Wang, B. G., Tang, X. Z., Hou, H. M., and Yuan, Y. R. (1993). A preliminary study on the magnetostratigraphy in waters of Nansha Islands. *Topic Oceanol.* 12, 53–60 (in Chinese with English abstract).

Wang, J. T. (1989). Study on geochemistry and geochemical classification of elements B, F, Rb and Sr in Yellow Wea (Huanghai Sea) sediment. *Oceanol. Limnol. Sinica* 20, 517–527 (in Chinese with English abstract).

Wang, L., Sarnthein, M., Erlenkeuser, H., Grimalt, J., Grootes, P., Heilig, S., et al. (1999). East Asian monsoon climate during the late plestocene: high-resilution sediment records from the South China Sea. *Mar. Geol.* 156, 245–284. doi: 10.1016/S0025-3227(98)00182-0

Wang, P. X. (2009). Toward scientific breakthrough in the South China Sea. *J. Trop. Oceanogr.* 28, 1–4 (in Chinese with English abstract).

Wang, P. X., Wang, L. J., Bian, Y. H., and Jian, Z. M. (1995). Late quaternary paleoceanography of the South China Sea: surface circulation and carbonate cycles. *Mar. Geol.* 127, 145–165. doi: 10.1016/0025-3227(95)00008-M

Wang, X. M., Xia, D. S., Zhang, C. X., Lang, L. L., Hua, T., and Zhao, S. (2012). Geochemical and magnetic characteristics of fine-grained surface sediments in potential dust source areas: implications for tracing the provenance of Aeolian deposits and associated palaeoclimatic change in East Asia. *Palaeogeogr. Palaeoclimatol. Palaeoecol.* 323, 123–132. doi: 10.1016/j.palaeo.2012.02.005

Wei, G. J., Liu, Y., Ma, J. L., Xie, L. H., Chen, J. F., Deng, W. F., et al. (2012). Nd, Sr isotopes and elemental geochemistry of surface sediments from the South China Sea: implications for provenance tracing. *Mar. Geol.* 319–322, 21–34. doi: 10.1016/j.margeo.2012.05.007

Wei, G. J., Li, X. H., Liu, Y., Shao, L., and Liang, X. R. (2006). Geochemical record of chemical weathering and monsoon climate change since the early Miocene in the South China Sea. *Paleoceanography* 21, PA4214. doi: 10.1029/2006PA001300

Wei, K. Y., Yang, T. N., and Huang, C. Y. (1997), Glacial Holocene calcareous nannofossils and paleoceanography in the northern South China Sea. *Mar. Micropal.* 32, 95–114. doi: 10.1016/S0377-8398(97)00015-7

Wronkiewicz, D. J., and Condie, K. C. (1987). Geochemistry of Archean shales from the witwatersrand supergroup, South Africa: source-area weathering and provenance. *Geochim. Cosmochim. Ac.* 51, 2401–2416. doi: 10.1016/0016-7037(87)90293-6

Xu, F. J., Li, A. C., Li, T. G., Meng, Q. Y., Chen, S. Y., Lin, C. Y., et al. (2011). The paleoenvironmental significance of magnetic susceptibility of sediments on the East China Sea inner shelf since the last deglaciation. *Acta Oecanol. Sinica* 33, 91–97 (in Chinese with English abstract).

Yang, X. Q., Zhou, W. J., Gao, F. L., and Li, H. M. (2007). Remanence magnetic records of the recent 130000 years from the sediments in Nansha area, South China Sea. *Front. Earth Sci. China* 1:80. doi: 10.1007/s11707-007-0011-8

Yim, W. W. S., Huang, G., and Chan, L. S. (2004). Magnetic susceptibility study of late quaternary inner continental shelf sediments in the Hongkong SAR, China. *Quatern. Int.* 117, 41–54. doi: 10.1016/S1040-6182(03)00115-0

Yokoyama, Y., Suzuki, A., Siringan, F., Maeda, Y., Abe-Ouchi, A., Ohgaito, R., et al. (2011). Mid-Holocene palaeoceanography of the northern South China Sea using coupled fossil-modern coral and atmosphere-ocean GCM model. *Geophys. Res. Lett.* 38, L00F03. doi: 10.1029/2010gl044231

Yu, L. Z., and Oldfield, F. (1989). A multivariate mixing model for identifying sediment source from magnetic measurements. *Quaternary Res.* 32, 168–181. doi: 10.1016/0033-5894(89)90073-2

Zan, J. B., Fang, X. M., Yan, M. D., Zhang, W. L., and Zhang, Z. G. (2015). Magnetic variations in surface soils in the NE Tibetan Plateau indicating the climatic boundary between the Westerly and East Asian summer monsoon regimes in NW China. *Global Planet. Change* 130, 1–6. doi: 10.1016/j.gloplacha.2015.03.008

Zhang, C. X., Paterson, G. A., and Liu, Q. S. (2012). A new mechanism for the magnetic enhancement of hematite during heating: the role of clay minerals. *Stud. Geophys. Geodaet.* 56, 845–860. doi: 10.1007/s11200-011-9018-4

Zhang, J. Y., Gao, H. F., Peng, X. C., Zhang, Y. L., and Wang, Y. M. (2010). Comparison of magnetic susceptibility of late quaternary sediment derived from slopes in the South China Sea and implication for paleoceanography. *Mar. Geol. Quatern. Geol.* 30, 151–164. doi: 10.3724/SP.J.1140.2010.04151 (in Chinese with English abstract).

Zhang, Q., Xiao, M. Z., Singh, V. P., Liu, L., and Xu, C. Y. (2015). Observational evidence of summer precipitation deficit-temperature coupling in China. *J. Geophys. Res.* 120, 10040–10049. doi: 10.1002/2015jd023830

Zhao, Y. Y., and Yan, M. C. (1994). *Geochemistry of Sediments of Shallow Seas of China*. Beijing: Science Press.

Conflict of Interest Statement: The authors declare that the research was conducted in the absence of any commercial or financial relationships that could be construed as a potential conflict of interest.